Supplementary Information (SI) for ChemComm.

Supplementary Information

CO_2-mediated hydrogen storage and release cycles realized by bimetallic ruthenium complex in pure water

Tianhua Cui,[a] Huihua Gong,[b] Li Ji,[c] Yuxuan Kong,[d] Siheng Yang,[a] Weichao Xue,[a] Xueli Zheng,[a] Haiyan Fu,[a] Chong Cheng,[d] Shuang Li,[d] Hua Chen,[a] Ruixiang Li,[*, a] Jiaqi Xu,[*, a, e]

a. Key Laboratory of Green Chemistry and Technology of Ministry of Education, College of Chemistry, Sichuan University, Chengdu, Sichuan 610064, China.
b. Analytical and Testing Center, College of Chemistry and Chemical Engineering, Neijiang Normal University, Neijiang 641112, P. R. China
c. Sichuan Research Institute of Chemical Quality and Safety Testing, Chengdu, Sichuan 610031, P.R. China
d. College of Polymer Science and Engineering, State Key Laboratory of Polymer Materials Engineering, Sichuan University, Chengdu, 610065, P. R. China
e. Laboratory of Photonics and Interfaces, École Polytechnique Fédérale de Lausanne, 1015 Lausanne, Switzerland

E-mail: jqxu@scu.edu.cn, jiaqi.xu@epfl.ch, jq-xu@qq.com (J. Xu)
liruixiang@scu.edu.cn (R. Li)

General: NMR spectra were recorded on a Bruker AVII-400 spectrometer at 400 MHz for ^1H NMR and 162 MHz for ^{31}P NMR. Chemical shifts were reported in ppm with Me_4Si as internal standard for ^1H NMR and 85% H_3PO_4 as external standard for ^{31}P NMR.

All the solvents used for reactions were distilled under argon after drying over an appropriate drying agent. All other commercially available reagents were purchased from Aaladin, Adamas, Aldrich, and Alfa Aesar Chemical Company.

We thank Comprehensive Training Platform of the Specialized Laboratory in the College of Chemistry at Sichuan University and Analytical & Testing Center of Sichuan University for the support.

Catalytic hydrogenation of CO_2:

Catalytic CO_2 hydrogenation was carried out in a Hastelloy Autoclave Reactor of 25 mL. The catalyst was dissolved in a degassed pure water (10 mL). The reactor was purged with high pure N_2 for three times, and then pressurized with CO_2/H_2 (1:25) of total pressure 26 bar and heated at 30-140 °C for the desired time. Formic acid (FA) was quantified by ^1H NMR spectroscopy with D_2O as the solvent and DMF as internal standard.

To explore the underlying mechanism, stoichiometric reactions were conducted with 30 μmol Ru-NNN complex **1** under CO_2/H_2 (CO_2: H_2 = 1: 25) of total pressure 26 bar in the mixture solvent of CD_3CN and D_2O (2 mL: 2 mL) at 80 °C. The reaction intermediates were monitored in-situ by NMR.

Catalytic formic acid (FA) dehydrogenation:

FA dehydrogenation was carried out in a Hastelloy Autoclave Reactor of 25 mL. The catalyst was dissolved in a degassed pure water (1.9 mL) and FA (0.1 mL). The reactor was purged with high pure N_2 for three times and was heated at 30-80 °C for the desired time. Then, the unreacted FA was quantified by ^1H NMR spectroscopy with DMF as internal standard and D_2O as the solvent.

Ru-catalyzed H_2 storage and release cycles

Catalytic CO_2 hydrogenation was carried out in a Hastelloy Autoclave Reactor of 50 mL. 20 μmol complex **1** was dissolved in a degassed D_2O (20 mL). The reactor was pressurized with CO_2/H_2 (1:50) of total pressure 51 bar and heated at 80 °C for 8 h. At the end of hydrogenation of CO_2, the pressure of the reactor is released and FA dehydrogenation is carried out at the condition of 80 °C. The unreacted FA was quantified by ^1H NMR spectroscopy with DMF as internal standard and D_2O as the solvent.

Product analysis:

The gas products were qualitatively and quantitatively analyzed using gas chromatography (GC, PANNA GC-A60). The GC is equipped with two detectors: a thermal conductivity detector (TCD) and a flame ionization detector (FID).

For gas analysis, N_2 was used as the carrier gas for TCD to detect H_2, while FID was employed to detect CO_2. A methanizer is equipped in the GC system to convert CO_2 and CO into CH_4 prior to detection by FID detector.

In-situ FTIR measurements

In-situ FTIR spectra were recorded with a Nicolet iS50 spectrometer equipped with an MCT detector. The complex **1** was solved in the mixture solvent of FA and H_2O. After purging with N_2 for half an hour, the background spectrum was measured under a N_2 atmosphere at room temperature. The *in-situ* FTIR were monitored in real-time with a time resolution of 10 min per spectrum at room temperature.

Calculations of TONs and TOFs:

$$TON_{hydrogenation} = \frac{n_{FA}}{n_{cat}}$$

$$TON_{dehydrogenation} = \frac{n_{FA} - n_{unreacted\ FA}}{n_{cat}}$$

$$TOF_{hydrogenation} = \frac{TON_{hydrogenation}}{t}$$

$$TOF_{dehydrogenation} = \frac{TON_{dehydrogenation}}{t}$$

$$Standard\ Deviation: \sigma = \sqrt{\frac{\sum_{i=1}^{n}(x_i - \mu)^2}{n}}$$

The TON was calculated based on the mean value derived from 3 independent replicate experiments.

A complete hydrogenation-dehydrogenation cycle proceeds as follows:

1. **System Setup**: The solution and catalyst were loaded into the reactor, followed by purging with CO_2 to displace residual air.
2. **Hydrogenation Step**: The reactor was pressurized to the standard hydrogenation conditions ($H_2 : CO_2 = 2.5$ Mpa : 0.1 Mpa) and heated to the target temperature (e.g. 80 °C) to initiate CO_2 hydrogenation. Upon reaction completion, the system was cooled to room temperature.
3. **Gas Management**: Then venting of residual gases was performed after the reactor was cooled to 25 °C. Then, high-pressure N_2 gas was carefully vented, and the reactor was purged with N_2 to remove residual H_2 and CO_2.
4. **Dehydrogenation Step**: The reactor was sealed and heated to the dehydrogenation temperature (e.g. 80 °C) under ambient pressure to trigger formic acid decomposition.
5. **Cycle Repetition**: Steps 2-4 are repeated for subsequent cycles.

Preparation and characterization of ligands and complexes

The synthesis of ligands: Pyridine 2,6-dicarboxylate (15 g) and anhydrous ethanol (120 mL) were added into a round-bottom flask of 250 mL equipped with a reflux condenser, and then acetyl chloride of 25 mL was slowly dropped to the alcohol solution. The mixture solution reacted at room temperature for 24 hours. Upon completion of the reaction, the solid was removed by filtration, and the filtrate was neutralized with sodium carbonate solution, then extracted with ethyl acetate to yield white solid diethyl pyridine 2,6-dicarboxylate. Subsequently, the diethyl pyridine 2,6-dicarboxylate and ethanol sodium (8.8 g) were added to the flask containing toluene of 60 mL in an ice bath, followed by the addition of a toluene solution of acetone (8.7 mL) to produce a yellowish turbid mixture. The reaction proceeded at room temperature for 12 hours. At the end of reaction, the mixture was filtered to collect a light yellow solid. And then the solid was neutralized to pH=1 with dilute hydrochloric acid before being extracted with ethyl acetate to obtain 1,1'-(pyridine-2,6-diyl) bis(butane-1,3-dione). Subsequently, 1,1'-(pyridine-2,6-diyl)bis(butane-1,3-dione) (2 mmol), glacial acetic acid (4 mL), and ethanol (30 mL) were added in a round-bottom flask of 100 mL and the mixture solution was stirred at room temperature for 30 minutes, followed by the addition of an ethanolic solution containing 4 mmol of hydrazine hydrate via a pressure-equalizing dropping funnel. Then the temperature was raised to 65 °C and continued to react for 24 hours. Upon completion, the solution was concentrated to around 10 mL under vacuum evaporation, neutralized to pH=8 with sodium carbonate solution, and extracted with ethyl acetate to yield faint yellow solid **L-NNN**.

The ligands **L-NNN-Me** and **L-NNN-Et** were prepared by replacing hydrazine hydrate with equivalent amounts of methylhydrazine and ethylhydrazine under identical reaction conditions.

The synthesis of complex 1: A mixture of ligand **L-NNN** (1 mmol) and $RuCl_3 \cdot 3H_2O$ (1 mmol) was refluxed in EtOH (60 mL) for 5 hours to give reddish-brown solid. The solid was filtered, washed with diethyl ether, and dried under vacuum. Furthermore, the alcohol solution (30 mL) of the reddish-brown solid reacted with PPh_3 (1 mmol) in the presence of Et_3N (1 mL) under the condition of refluxing for 6 hours. After completion of the reaction, the solvent was removed under vacuum to get a reddish-brown solid. The resulting solid was dissolved in DCM and filtered to remove insoluble impurities and yield a red solution. Upon addition of ether to the solution, dark red orange solid complex **1** was crystallized from the solution with a yield of 50%. ^1H NMR (400 MHz, Acetonitrile-d_3) δ 7.45 – 7.22 (m, 20H), 7.21 – 7.06 (m, 12H), 7.00 (d, J = 7.9 Hz, 2H), 6.86 (d, J = 7.9 Hz, 2H), 6.45 (s, 2H), 5.83 (s, 2H), 2.51 (s, 6H), 1.04 (s, 6H). ^{31}P NMR (162 MHz, Methylene Chloride-d_2) δ 47.7. The HRMS displayed the exact molecular ion peak of $[M_2–Cl]^+$ ($C_{62}H_{54}ClN_{10}P_2Ru_2^+$) at m/z 1239.1798(Exact Mass: 1239.1784).

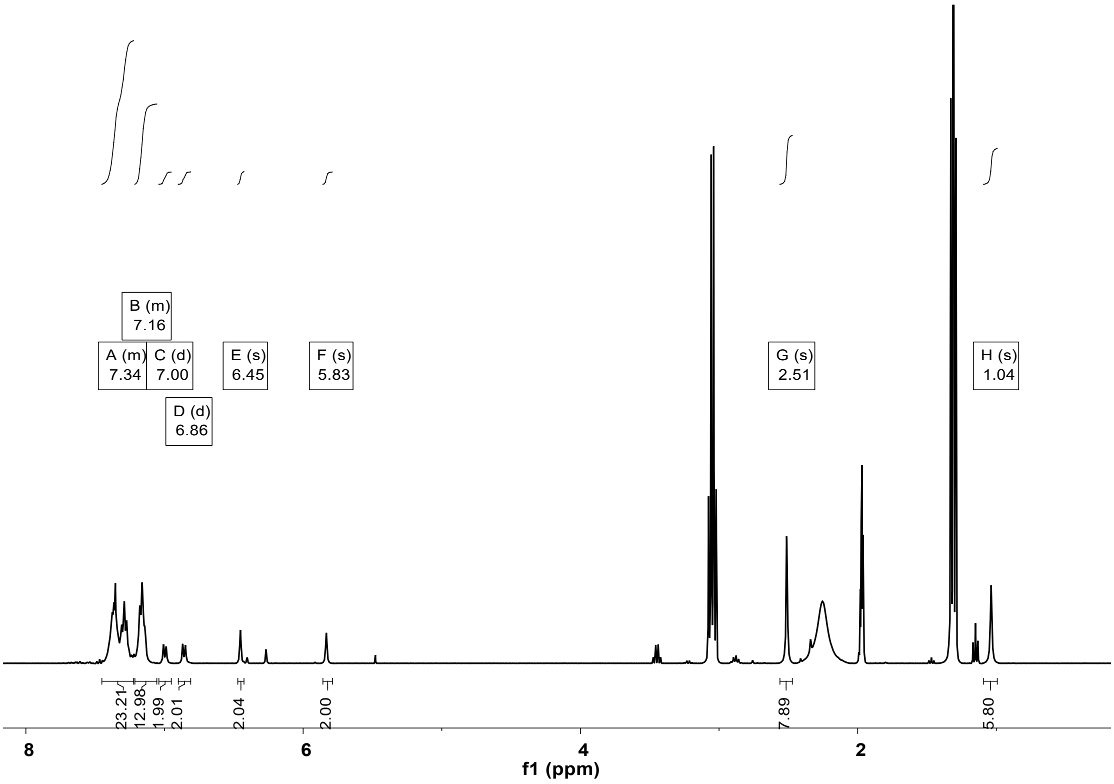

Figure S1. ^{1}H NMR spectrum of complex **1** (400 MHz, Acetonitrile-d_3).

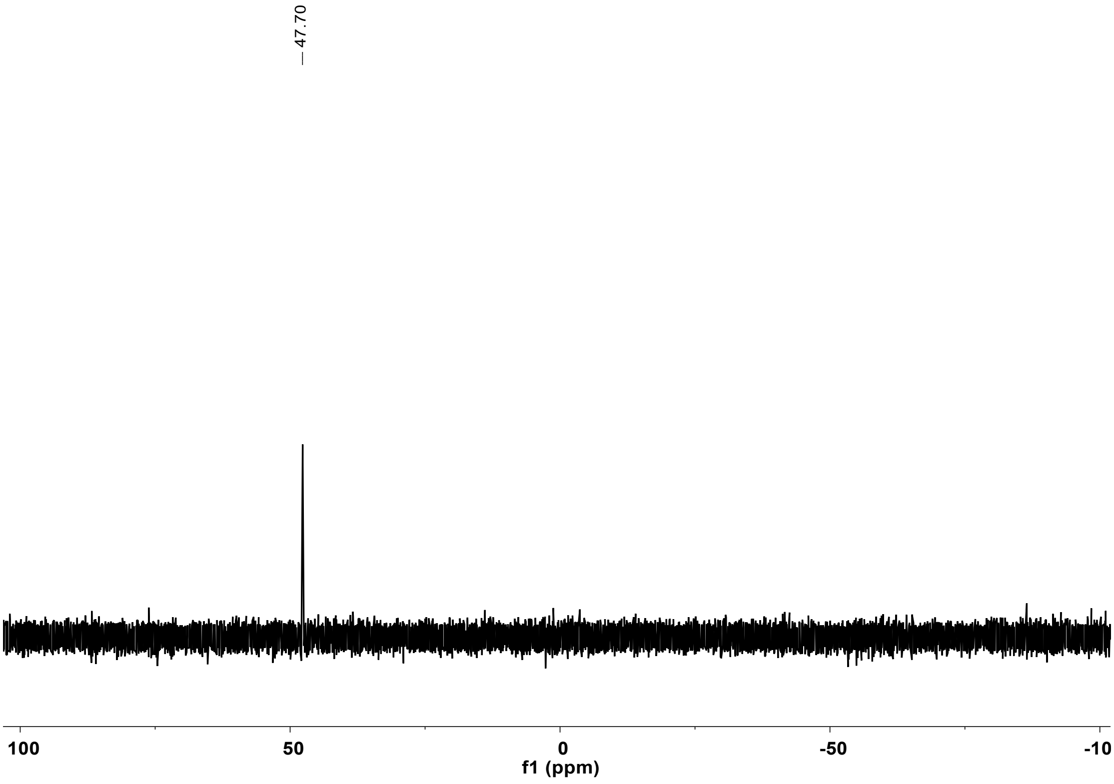

Figure S2. ^{31}P NMR spectrum of complex **1** (162 MHz, Methylene Chloride-d_2).

X-ray single crystal data of complex 1

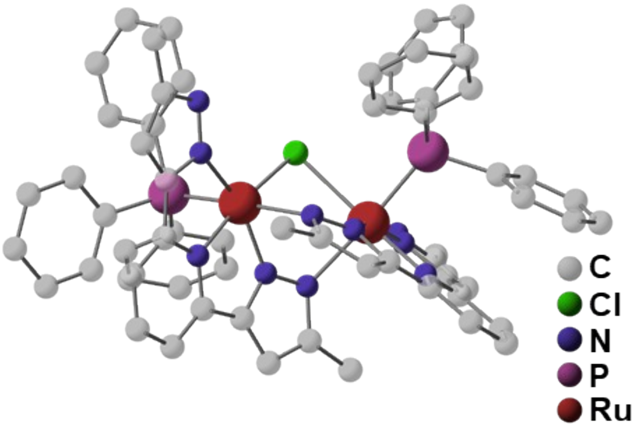

Figure S3. X-ray single crystal data of complex **1.** (CCDC number: 2393346)

Identification code	150115_s1_zz_m
Empirical formula	$C_{63}Cl_3N_{10}O_3P_2Ru_2H_{0.5}$
Formula weight	1315.66
Temperature/K	144(3)
Crystal system	triclinic
Space group	P-1
a/Å	14.329
b/Å	15.702
c/Å	20.016
α/°	105.32
β/°	97.25
γ/°	107.06
Volume/Å^3	4050.0
Z	2
ρ_{calc}g/cm^3	1.079
m/mm^{-1}	0.551
F(000)	1283.0
Crystal size/mm^3	0.3 × 0.2 × 0.2
Radiation	MoKα (λ = 0.71073)
2Θ range for data collection/°	5.818 to 52.746°
Index ranges	$-17 \le h \le 17$, $-19 \le k \le 19$, $-25 \le l \le 24$
Reflections collected	37749
Independent reflections	16506 [R_{int} = 0.0348, R_{sigma} = 0.0616]
Data/restraints/parameters	16506/0/761
Goodness-of-fit on F^2	1.109
Final R indexes [I>=2σ (I)]	R_1 = 0.0622, wR_2 = 0.1633
Final R indexes [all data]	R_1 = 0.0852, wR_2 = 0.1773
Largest diff. peak/hole / e Å^{-3}	1.54/-0.90

Figure S4. HRMS of complex **1. (**Exact Mass: 1239.1784 found:1239.1798)

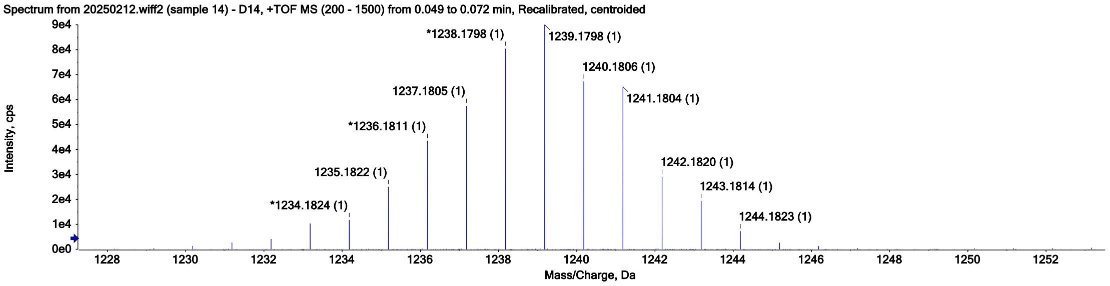

The synthesis of complex 2: A mixture of ligand **L-NNN-Me** (1 mmol) and $RuCl_3•3H_2O$ (1 mmol) was refluxed in EtOH (60 mL) for 5 hours to give reddish-brown precipitate. The solid was filtered, washed with diethyl ether, and dried under vacuum. Furthermore, the alcohol solution (30 mL) of the reddish-brown solid reacted with PPh_3 (1 mmol) in the presence of Et_3N (1mL) under the condition of refluxing for 6 hours. After completion of the reaction, the solvent was removed under vacuum to get a reddish-brown solid. The resulting solid was dissolved in DCM, followed by filtration to remove insoluble impurities, yielding a red solution. Upon addition of ether to the solution, orange solid complex **2** was crystallized from the solution with a yield of 54%. ^{1}H NMR (400 MHz, Methylene Chloride-d_2) δ 7.35 – 7.28 (m, 1H), 7.25 – 7.15 (m, 3H), 7.13 (d, J = 7.9 Hz, 2H), 7.09 – 6.97 (m, 12H), 6.51 (s, 2H), 3.94 (s, 6H), 2.28 (s, 6H). ^{31}P NMR (162 MHz, Methylene Chloride-d_2) δ 44.2.

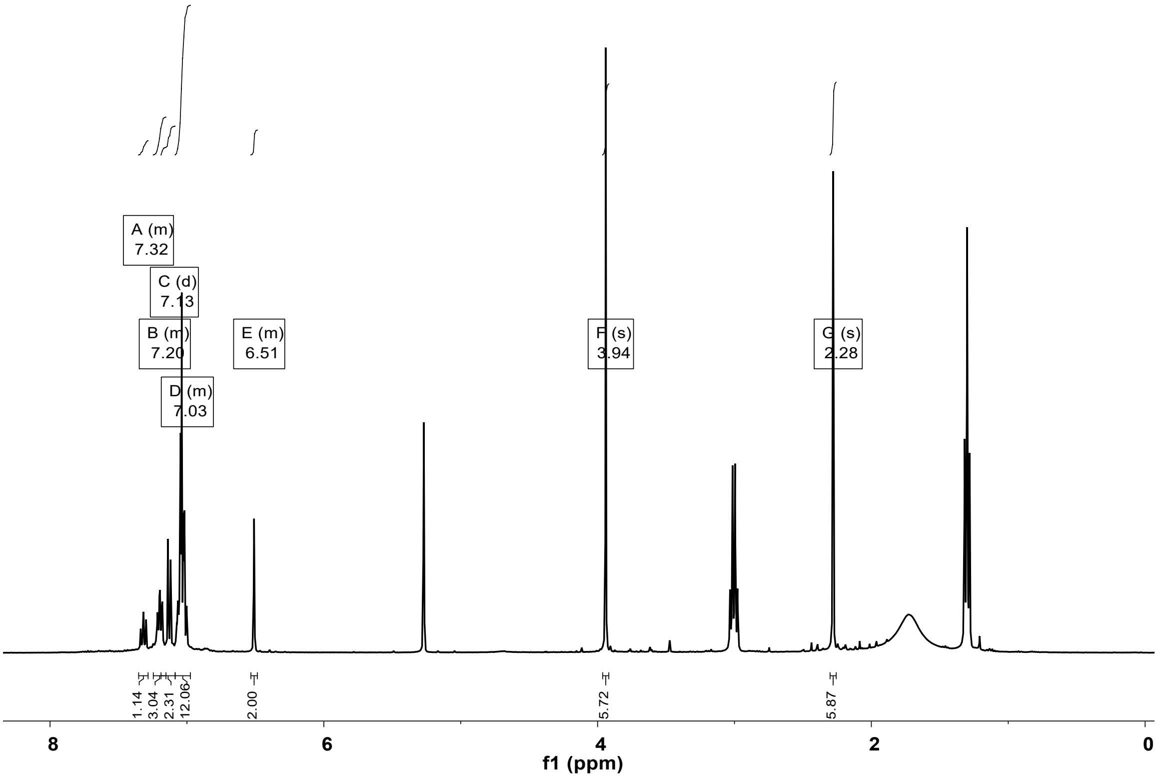

Figure S5. ^{1}H NMR spectrum of complex **2** (400 MHz, CD_2Cl_2).

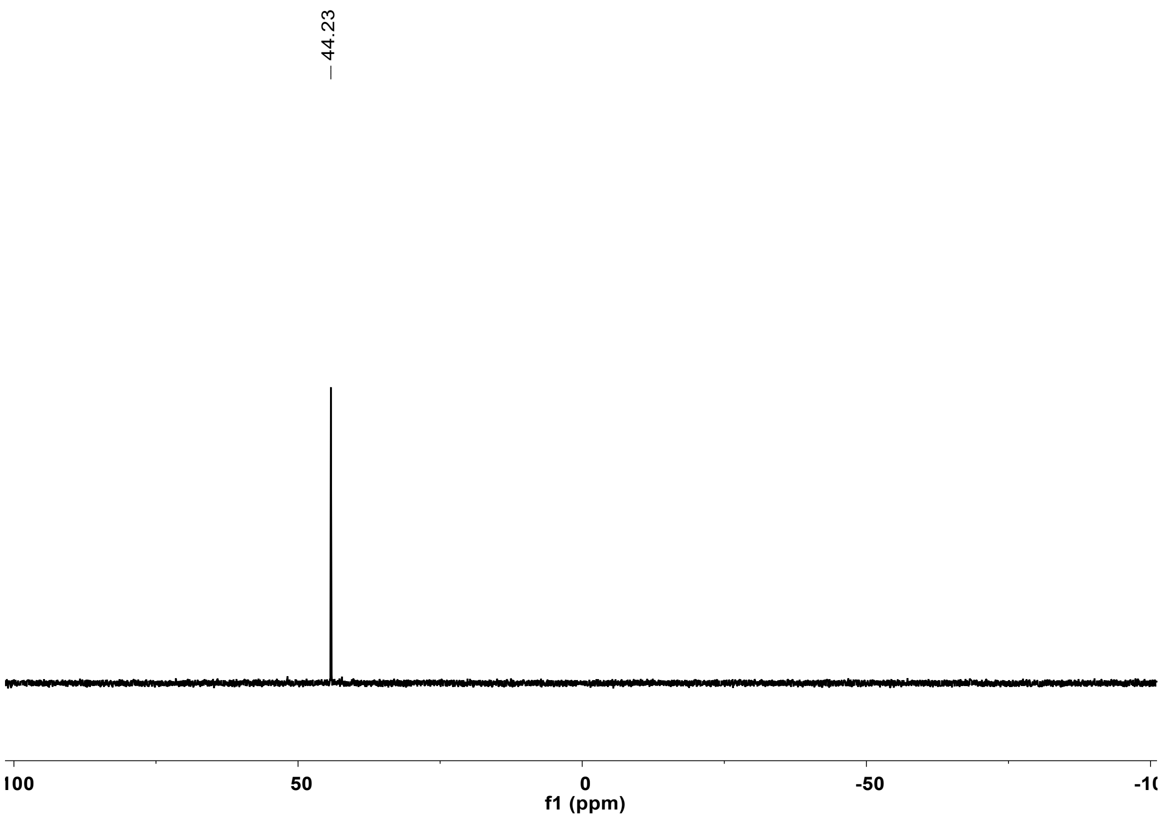

Figure S6. ^{31}P NMR spectrum of complex **2** (162 MHz, CD_2Cl_2).

The synthesis of complex 3: A mixture of ligand **L-NNN-Et** (1 mmol) and $RuCl_3$•$3H_2O$ (1 mmol) was refluxed in EtOH (60 mL) for 5 hours to give reddish-brown precipitate. The solid was filtered, washed with diethyl ether, and dried under vacuum. Furthermore, the alcohol solution (30 mL) of the reddish-brown solid reacted with PPh_3 (1 mmol) in the presence of Et_3N (1mL) under the condition of refluxing for 6 hours. After completion of the reaction, the solvent was removed under vacuum to get a reddish-brown solid. The resulting solid was dissolved in DCM, followed by filtration to remove insoluble impurities, yielding a red solution. Upon addition of ether to the solution, orange solid complex **3** was crystallized from the solution with a yield of 61%. ^{1}H NMR (400 MHz, Chloroform-*d*) δ 7.69 – 7.63 (m, 1H),7.44 (d, J = 7.9 Hz, 2H), 7.25 – 7.19 (m, 3H), 7.11 – 7.01 (m, 12H), 6.55 (s, 2H), 3.44 (s, 4H), 3.23 (s, 6H), 2.07 (s, 6H). ^{31}P NMR (162 MHz, Chloroform-*d*) δ 43.0.

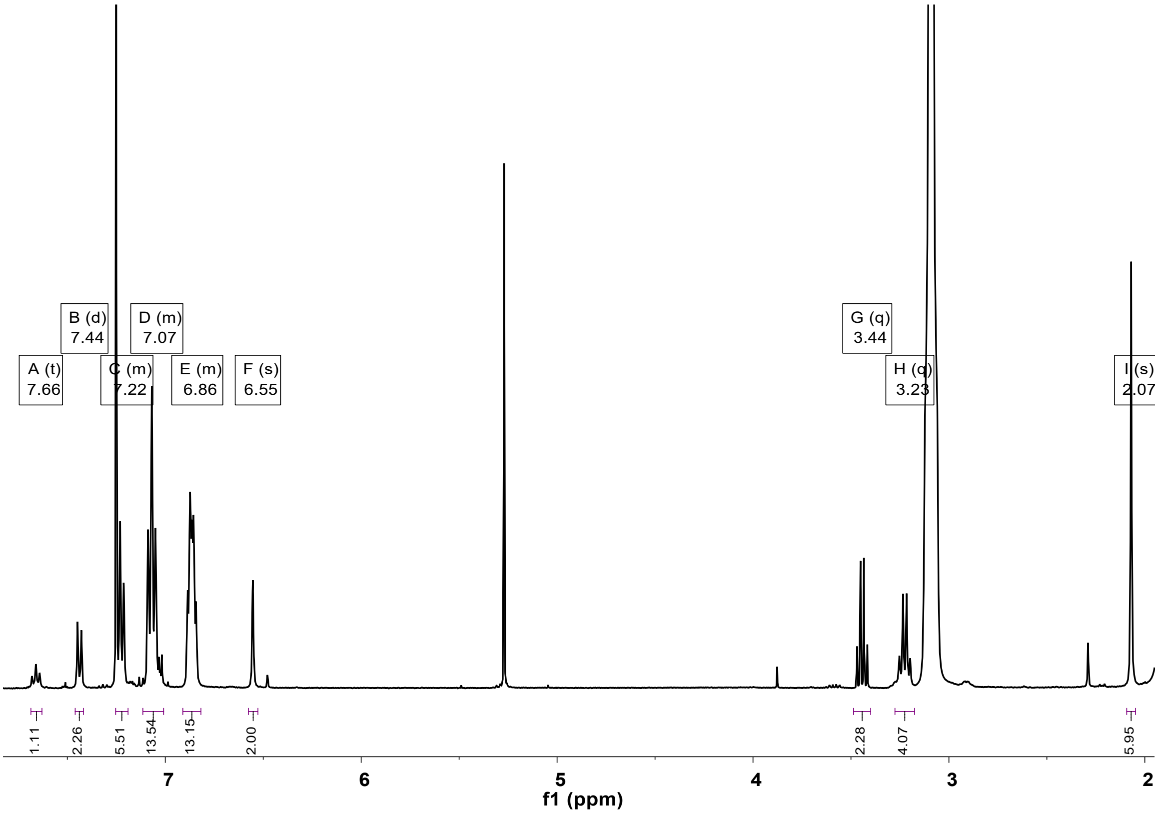

Figure S7. ^{1}H NMR spectrum of complex **3** (400 MHz, CD_2Cl_2)**.**

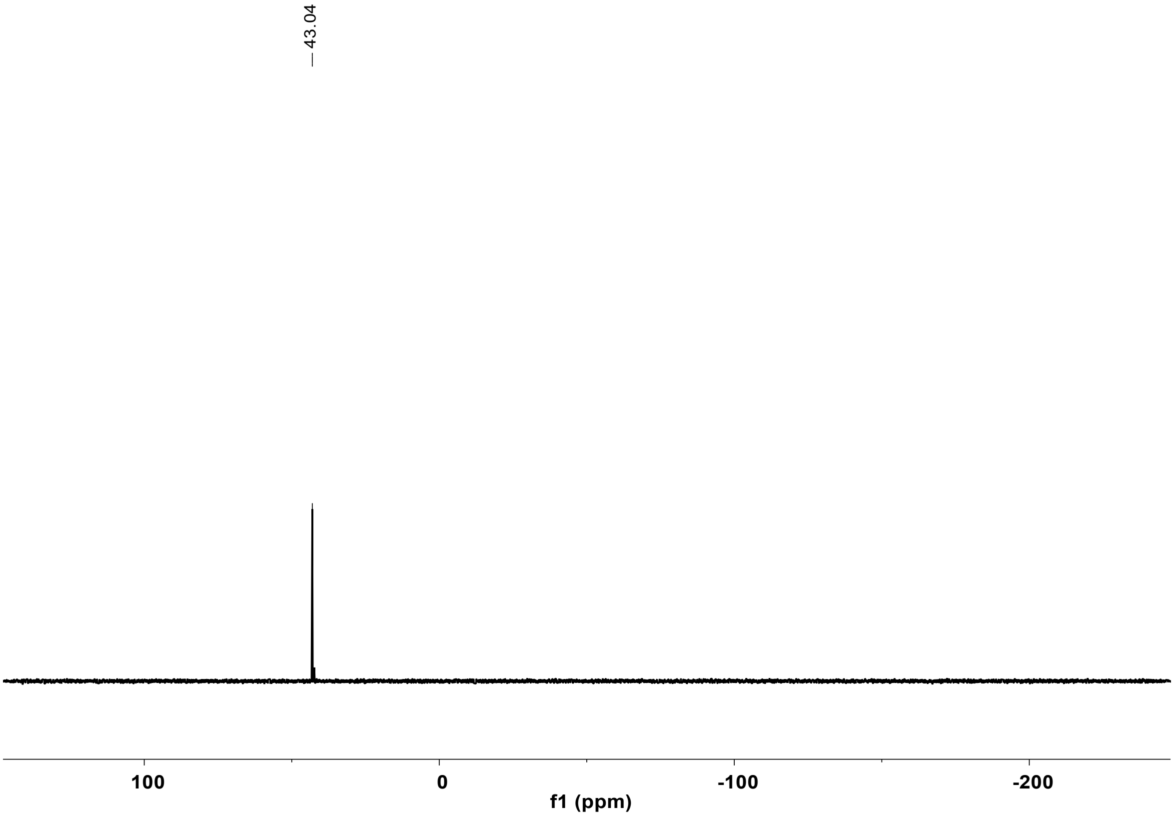

Figure S8. ^{31}P NMR spectrum of complex **3** (162 MHz, CD_2Cl_2).

X-ray single crystal data of complex 3

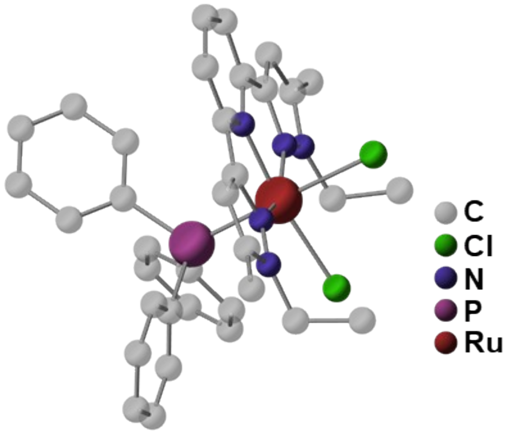

Figure S9. X-ray single crystal data of **3.** (CCDC number: 2393349)

Identification code	211129_s1_cth
Empirical formula	$C_{35}H_{36}Cl_2N_5PRu$
Formula weight	729.63
Temperature/K	293.15
Crystal system	orthorhombic
Space group	$P2_12_12_1$
a/Å	10.7554(4)
b/Å	16.9347(6)
c/Å	18.5184(7)
α/°	90
β/°	90
γ/°	90
Volume/Å^3	3372.9(2)
Z	4
ρ_{calc}g/cm^3	1.437
μ/mm^{-1}	0.703
F(000)	1496.0
Crystal size/mm^3	0.35 × 0.3 × 0.25
Radiation	MoKα (λ = 0.71073)
2Θ range for data collection/°	5.806 to 52.744
Index ranges	$-13 \leq h \leq 10$, $-21 \leq k \leq 18$, $-9 \leq l \leq 23$
Reflections collected	10692
Independent reflections	6355 [R_{int} = 0.0275, R_{sigma} = 0.0570]
Data/restraints/parameters	6355/0/401
Goodness-of-fit on F^2	1.052
Final R indexes [I>=2σ (I)]	R_1 = 0.0380, wR_2 = 0.0829
Final R indexes [all data]	R_1 = 0.0491, wR_2 = 0.0898
Largest diff. peak/hole / e Å^{-3}	0.67/-0.56
Flack parameter	-0.03(2)

Table S1. Reported catalytic systems (References 1-10) utilizing formic acid as a liquid hydrogen carrier (LHCs).[1–10]

Catalysts	Solvent of hydrogenation	Additives	Solvent of dehydrogenation	Additives	Cycle times/ M(total)	CO_2/H_2 (MPa) pressure for hydrogenation	Ref.
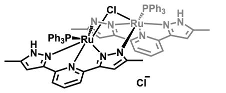	H_2O		H_2O		15/ 2 mmol	0.1/2.5	This work
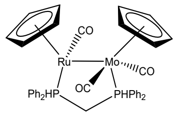	C_6H_6	NEt_3	THF		1/ 0.387 mmol	3/3	1
$[RuCl_2(mTPPMS)_2]_2$	H_2O	$NaHCO_3$	H_2O	HCOONa	3/ 0.771 mmol	0.1/10	2
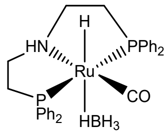	THF/H_2O	NaOH	Dioxane/H_2O	HCOONa	6/ 102 mmol	3/3	3
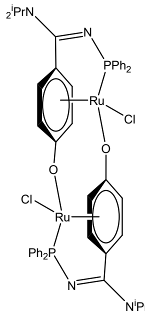	DMSO		DMSO		4/ 10.49 mmol	3/3	4
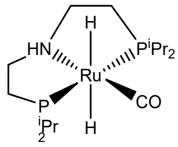	EMIMOAc		BMIMOAc		13/ 386 mmol	1/2	5
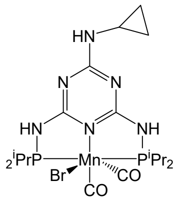	H_2O/THF	Lysine	H_2O/THF		10/ 50 mmol	2/6	6
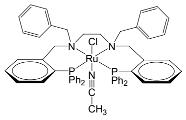	DBU		Tol		5/ 408 mmol	7/7	7

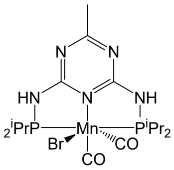	H_2O/THF	$KHCO_3$ Lys	H_2O/THF		5/ 20.6 mmol	0.1/6	8
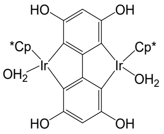	H_2O/THF	$KHCO_3$	H_2O	HCO_2Na	2/ 4.3 mmol	2/2	9
$[RuCl_2(benzene)]_2$ /6 eq. 1,2-bis(diphenylphosphino) ethane	DMF	NEt_3	*N*,*N*-dimethylhexylamine		8/ 676 mmol	3/3	10

As revealed by Table S1, most FA-based hydrogen storage systems require additional additives or organic solvents, whereas our system can operate in pure water without any additives (mild and environmentally friendly conditions).

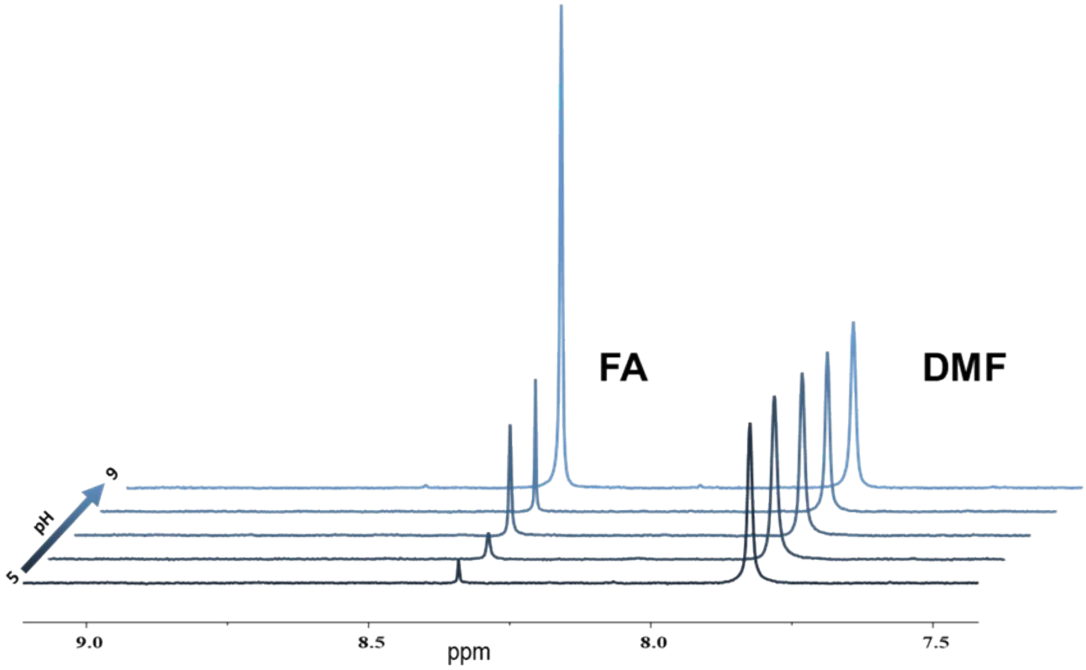

Figure S10. CO_2 hydrogenation with complex **1** in different pH buffer.

Although a basic condition can significantly improve the CO_2 hydrogenation performance of complex **1**, it also induces other problems such as increased energy consumption for base regeneration. So, wo try to avoid the use of bases. Notably, complex **1** can also catalyze CO_2 hydrogenation in acidic buffer solutions, which explain its CO_2 hydrogenation performance in pure water (the dissolution of CO_2 and the formation of FA will cause the solution to become acidic).

Table S2. Ru catalysts for the hydrogenation of CO_2.

entry	cat. (μmol)	T (°C)	Formic acid			Standard Deviation
			[μmol]	TON	TOF (h^{-1})	
1	0.005	80	5.7	1130	141	0.5
2	0.01	80	6.3	628	79	0.5
3	1	80	8.5	8.5	1.1	0.4
4	10	80	29.0	2.9	0.4	4.3
5[b]	1	80	6.6	6.6	0.8	1.3
6[b]	1	80	12.6	12.6	1.6	1.2
7[b]	1	80	45.0	45	5.6	3.6
8[b]	1	80	92.0	92	11.5	7.4
9[b]	1	80	202	202	25	13
10	1	100	15.0	15	1.8	2.9
11	1	120	24.0	24	3	2.8
12[c]	0.01	30	3.7	372	2.3	0.4
13[d]	0.001	80	16.8	16900	1410	1.3
14[e]	1	80	0.9	0.9	0.1	0.1
15[f]	1	80	0.8	0.8	0.1	0.1
16[g]	1	80	2.3	2.3	0.3	0.2
17[h]	1	80	8.0	8.0	1.0	1.0
18[i]	1	80	23.4	23.4	1.0	1.4

[a] General conditions: T = 80 °C, complex **1** (1 μmol), $P(H_2) = 2.5$ MPa, $P(CO_2) = 0.1$ MPa, $V(H_2O) = 10$ mL, reaction time = 8 h; [b] pH = 5-9; [c] reaction time = 160 h; [d] $P(H_2)$ =7.5 Mpa, reaction time = 12 h; [e] complex **2**; [f] complex **3**; [g] CO_2 come from air; [h] use of aged complex **1**; [i] repeat hydrogenation experiments by successive CO_2/H_2 reloading cycles to the same batch without the dehydrogenation step. The TONs were calculated based on the mean value derived from 3 independent replicate experiments. The standard deviation was calculated based on the yields(μmol) of 3 independent replicate experiments.

Table S3. Ru catalysts for the HCOOH dehydrogenation.

entry	Cat. (μmol)	V_{FA}(mL)	T (°C)	TON	FA conversion	H_2 selectivity	H_2 yield (%)	Standard Deviation
1	1	0.1	80	387	14.6%	100%	14.6%	12
2	2	0.1	80	206	15.4%	101%	15.6%	16
3	3	0.1	80	225	25.6%	100%	25.6%	38
4	1	0.1	30	0	0	/	0	0
5	1	0.1	50	357	13.5%	100%	13.5%	6
6	1	0.01	80	67	26.1%	97%	25.3%	2
7	10	0.01	80	25	95.5%	101%	96.5%	29
8	1	0.1	80	387	14.6%	100%	14.6%	7
9	10	0.1	80	84	31.7%	100%	31.7%	64
10	1	1	80	5660	21.0%	102%	21.4%	60
11	10	1	80	613	23.2%	100%	23.2%	92
12	0	0.1	80	0	0	/	0	0

[a] General conditions: complex **1**, the total volume of FA and H_2O (V(total)) is 2 mL, reaction time = 24 h. H_2 yield (%) = FA conversion * H_2 selectivity. The TON was calculated based on the mean value derived from 3 independent replicate experiments. The standard deviation was calculated based on the yields(μmol) of 3 independent replicate experiments.

Table S4. Ru catalysts applied to H_2 storage and release cycles.

entry	Formic acid			Standard Deviation
	TON	H_2 storage [μmol]	H_2 release [μmol]	
1	7.0	140	140	5
2	6.9	137	137	2
3	6.4	128	128	6
4	6.7	134	134	3
5	6.5	130	130	5
6	6.2	124	124	4
7	6.5	129	129	4
8	6.7	134	134	5
9	6.1	122	122	4
10	6.6	132	132	3
11	6.4	128	128	6
12	6.4	127	127	7
13	5.8	116	116	9
14	7.3	146	146	9
15	6.8	136	136	5

[a] General conditions for hydrogenation: T = 80 °C, complex **1** (20 μmol), $P(H_2) = 6.0$ MPa, $P(CO_2) = 0.1$ MPa, $V(H_2O) = 20$ mL, reaction time = 8 h; General conditions for dehydrogenation: T = 80 °C, complex **1** (20 μmol), $P(H_2) = P(CO_2) = 0$ MPa, $V(H_2O) = 20$ mL, reaction time = 8 h; The TON was calculated based on the mean value derived from 3 independent replicate experiments. The standard deviation was calculated based on the yields(μmol) of 3 independent replicate experiments.

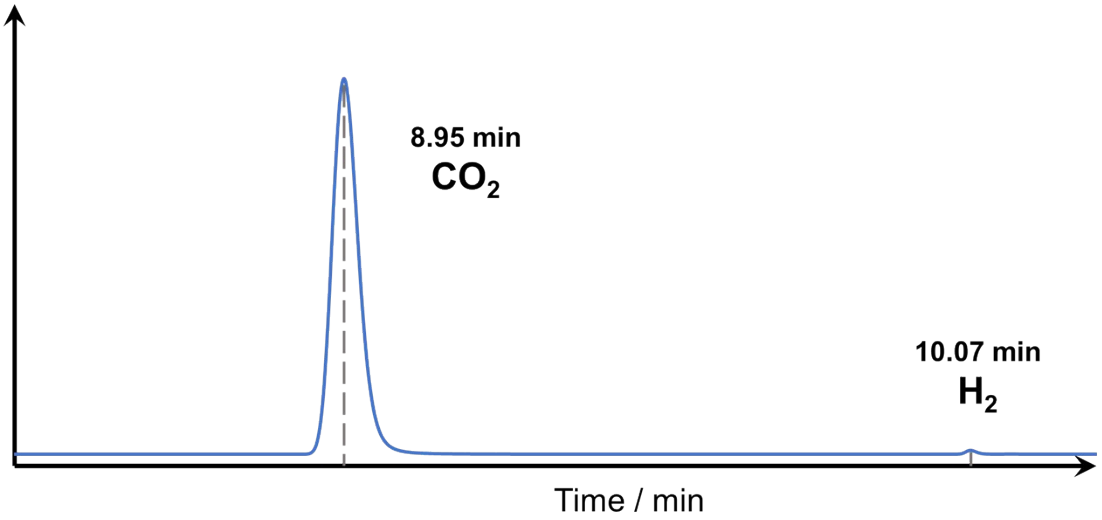

Figure S11. GC analysis of gaseous products after decomposition of FA. CO_2 is detected by an FID detector, while H_2 is detected by a TCD detector.

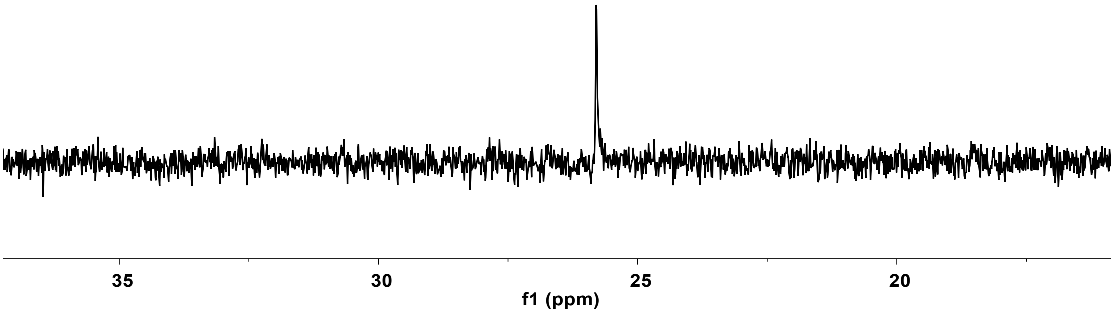

Figure S12. The ^{31}P NMR spectra of complex **1** solution after reaction.

The ^{31}P NMR spectra after reaction manifested that no free TPPO (29ppm) was detected in the liquid phase.

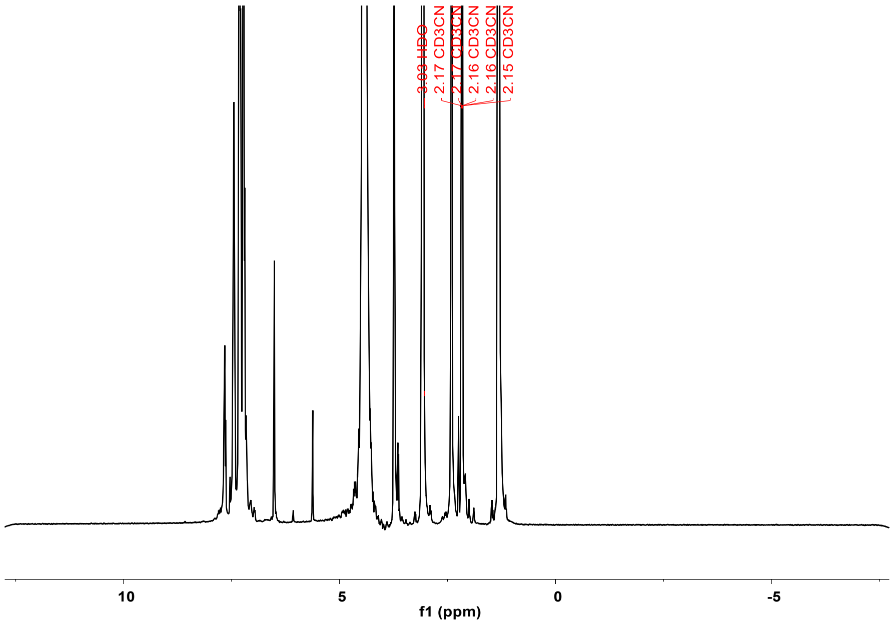

Figure S13. The ^1H NMR spectra of complex **1** solution after reaction.

DFT calculation details: Based on the aforementioned characterization, we hypothesized potential intermediates and calculated their Gibbs free energies, along with those of the transition states, using Gaussian 09[11] and Shermo[12]. The optimizations were performed with the SMD implicit solvent model at the B3LYP-D3(BJ)/def2-SVP level, and single-point energies were computed using the def2-TZVP basis set. The Gibbs free energies of the intermediates and transition states were calculated at T=353.15K and 1 atm using the Shermo program.

Table S5. Kinetic isotope effect (KIE) for FA dehydrogenation over complex 1.[a]

entry		**TOF**	**KIE**
1	H_2O+HCOOH	236	
2	D_2O+HCOOH	138	1.7
3	H_2O+DCOOD	102	2.3

[a] Reaction Conditions: HCOOH/DCOOD: D_2O/H_2O= 1mL:1mL, complex **1** (100 µmol), 80 °C. Initial TOF at 120 min. KIE = TOF (entry 1)/TOF (entry n) (n = 2, 3).

We observed kinetic isotope effect (KIE) in the isotope labelling studies. For instance, the reaction rate became much slower when HCOOH was replace by DCOOD or H_2O was replaced by D_2O during the formic dehydrogenation process. This indicates a dependency of the reaction on the concentration of H^+ ions, which aligns with the experimental results showing an increase in reaction rate with increasing FA concentration.

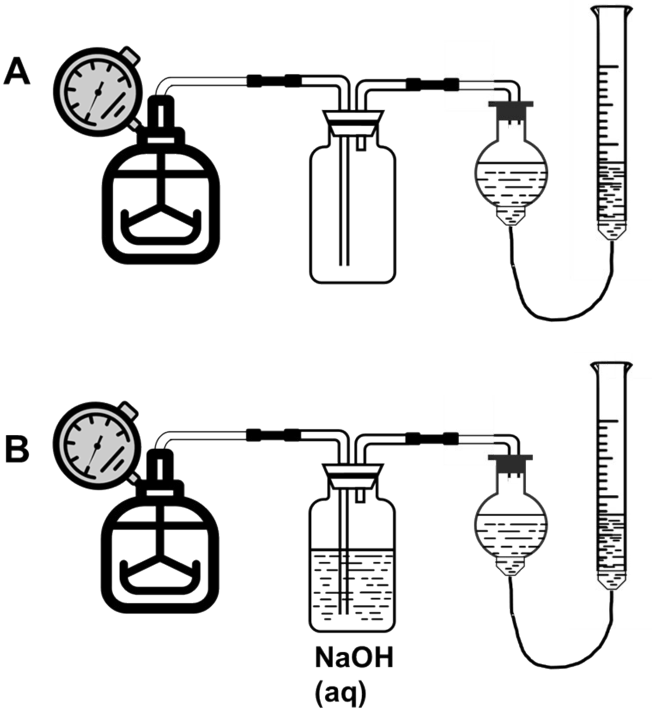

Figure S14. A device for measuring gas volume using the water displacement method. (A): Measuring the volume of CO_2 and H_2; (B): Measuring the volume of H_2.

Taking one dehydrogenation experiment as an example (Table S3, entry 10: Complex **1** = 1 μmol, V_{FA} = 1 mL, T = 80 °C, reaction time = 24 h), we further verified the volume of post-reaction gases by volumetric measurement (Figure S14). The experimental total volume of H_2 and CO_2 (246 mL) exhibited a 3.1% deviation from the theoretically calculated value (254 mL at STP), then we scrubbed the CO_2 component by passing the gas stream through NaOH solution, followed by volumetric measurement of residual H_2. The experimental hydrogen volume (125 mL) exhibited a 1.6% deviation from the theoretically calculated value (127 mL at STP).

Reference

1 M. Lok Man, Z. Zhou, S. Man Ng and C. Po Lau, *Dalton Trans.*, 2003, 3727–3735.

2 G. Papp, J. Csorba, G. Laurenczy and F. Joó, *Angew. Chem. Int. Ed.*, 2011, **50**, 10433–10435.

3 J. Kothandaraman, M. Czaun, A. Goeppert, R. Haiges, J.-P. Jones, R. B. May, G. K. S. Prakash and G. A. Olah, *ChemSusChem*, 2015, **8**, 1442–1451.

4 R. Verron, E. Puig, P. Sutra, A. Igau and C. Fischmeister, *ACS Catal.*, 2023, **13**, 5787–5794.

5 L. Piccirilli, B. Rabell, R. Padilla, A. Riisager, S. Das and M. Nielsen, *J. Am. Chem. Soc.*, 2023, **145**, 5655–5663.

6 D. Wei, R. Sang, P. Sponholz, H. Junge and M. Beller, *Nat. Energy*, 2022, **7**, 438–447.

7 S.-F. Hsu, S. Rommel, P. Eversfield, K. Muller, E. Klemm, W. R. Thiel and B. Plietker, *Angew. Chem. Int. Ed.*, 2014, **53**, 7074–7078.

8 D. Wei, X. Shi, P. Sponholz, H. Junge and M. Beller, *ACS Cent. Sci.*, 2022, **8**, 1457–1463.

9 J. F. Hull, Y. Himeda, W.-H. Wang, B. Hashiguchi, R. Periana, D. J. Szalda, J. T. Muckerman and E. Fujita, *Nat. Chem.*, 2012, **4**, 383–388.

10 A. Boddien , C. Federsel, P. Sponholz, D. Mellmann, R. Jackstell, H. Junge, G. Laurenczy and M. Beller, *Energy Environ. Sci.*, 2012, **5**, 8907-8911

11 M. Frisch, *et al.*, Gaussian, Inc., Wallingford CT, 2016.

12 T. Lu and Q. Chen, *Comput. Theor. Chem.*, 2021, **1200**, 113249.